

HT-FED2004-56822

UNSTEADY JETS IN CROSSFLOW

K. B. M. Q. Zaman
NASA Glenn Research Center
Cleveland, OH 44135

ABSTRACT

The effect of periodic perturbation on a jet in a cross-flow (JICF) is reviewed. In the first part of the paper, flow visualization results from several past works are discussed. Beginning with a description of the characteristic vortex systems of a JICF it is shown that specific perturbation techniques work by organizing and intensifying specific vortex systems. Oscillatory blowing works primarily through an organization of the shear layer vortices. A mechanical perturbation technique is found to organize the wake vortices. In the second part of the paper, results of an ongoing experiment involving another mechanical perturbation technique are discussed. It involves two tabs at the orifice exit whose asymmetry in placement is reversed periodically. It directly modulates the counter-rotating vortex pair (CVP). Effects of the perturbation for an array of three adjacent orifices are explored. The flowfield data show an improvement in mixing compared to the unperturbed case.

1. INTRODUCTION

A jet in a crossflow (JICF) occurs in numerous technological and propulsion applications. One of its usages has been in 'flow control' efforts. It has been explored for separation control in diffusers and over airfoils, for thrust vectoring with nozzle flows, for enhanced mixing in combustors as well as for secondary flow management in curved ducts. The majority of the research involved steady or continuous jets discharged into the crossflow. Research continues to focus on orifice geometry, orientation, array configuration and their placement. Lately, there is a growing interest in 'active control' by imparting a perturbation to the JICF.^{1,2} The interest stems from the promise of significantly larger benefit. For example, it has been shown in Ref. 1 that oscillatory blowing rather than steady blowing, from the same injection slot, is much more effective and efficient in controlling separation over a wing section.

It is fair to say that the fluid dynamics of a perturbed JICF is far from being clearly understood. The flowfield of a JICF with steady supply is already complex. There are various vortex systems with inherent unsteadiness.³ A given perturbation

technique apparently works through an organization and intensification of the vortices. In fact, different vortex systems of the flow may be energized by different techniques. Beginning with a description of the vortex systems of a JICF observed perturbation effects will be reviewed in §2 with the help of flow visualization pictures from several past investigations. In §3 results of a current experiment involving a mechanical perturbation technique will be presented. It employs a pair of oscillating 'tabs' at the exit of the orifice. As to be elaborated, this results in a direct modulation of the counter-rotating vortex pair (CVP) of the JICF. Results for an array of three orifices perturbed by the oscillating tabs will be presented.

2. VORTEX SYSTEMS OF A JICF AND EFFECT OF PERTURBATION

Several vortex systems can be identified in a JICF. This is illustrated in Fig. 1, reproduced from Ref. 3. The 'horse-shoe vortex', also called 'necklace vortex', occurs due to the reorientation of the approach boundary layer. The counter-rotating vortex pair (CVP), also referred to as the 'bound vortex pair', is a well-recognized and prominent feature of a JICF. The CVP has been known to persist hundreds of diameters from the origin. Both the horse-shoe vortex and the CVP have time-averaged definition, i.e., their signatures are detectable in the time-averaged flowfield. However, each may involve significant unsteadiness. The 'shear-layer vortices' and 'wake vortices' are intrinsically unsteady phenomena and detectable only in instantaneous snapshots of the flowfield.

The shear-layer vortices (or, alternatively, 'jet preferred mode vortices') are a result of the instability of the jet shear layer. Their dynamics are basically the same as studied extensively for free jets.⁴ With laminar efflux boundary layer there is initial roll up of the vortices with frequency scaling on the boundary layer thickness. Through successive amalgamation the frequency reduces to the 'preferred mode' Strouhal number of about 0.3, based on jet diameter, by the end of the potential core. It is also known that periodic forcing can directly organize the preferred mode vortices regardless of the initial boundary layer state.

The focus of Ref. 3 was on the wake vortices. These are similar to ‘Karman vortices’ shed from a bluff body – the column of jet, in this case, acting as the bluff body. However, as identified in Ref. 3, there are differences between the wake vortices and the shed vortices from a bluff body in origin as well as characteristics. The wake vortices will be discussed further in the following.

All vortex systems play a role in the dynamics of the JICF. It should be emphasized that these are not independent of each other. An effect on one may influence another. After all, the sources of all vorticity in a JICF are the efflux boundary layer of the orifice and the boundary layer on the wall from which the jet emerges. Yet, a given perturbation technique may primarily target a particular vortex system as elaborated next.

2.1 Oscillatory blowing:

The effect of oscillatory blowing or periodic forcing on an isolated JICF has been studied by several researchers in recent years.⁵⁻¹⁰ Profound impact on the flowfield has been observed. Figure 2 shows flow visualization pictures taken from Eroglu and Breidenthal.⁸ The picture at the top represents the steady case while that at the bottom is with forcing. The pulsation results in two branches of the jet, one penetrating deep into the crossflow.

In order to assess the effect on jet penetration, jet trajectories based on available correlation equations (see, e.g., Ref. 11) are shown by the dashed lines in Fig. 2. These are drawn approximately based on scales inferred from the photographs. For the unforced case, J represents the momentum flux ratio, $(U_j/U_\infty)^2$, where U_j is the jet velocity and U_∞ the freestream or crossflow velocity. It can be seen that the jet trajectory follows the correlation well. The case in the bottom picture involves square-wave pulsation with 100% modulation (i.e., the amplitude is varied between 0 and $2U_j$). Since for half the time the jet velocity is zero, a branch close to the wall is perhaps expected. Similarly, since for half the time the jet velocity is $2U_j$ a branch penetrating deeper than the unforced case is naturally expected. One might anticipate the deeper branch to correspond to a momentum flux ratio, $J_p = (2U_j/U_\infty)^2 = 4J$. Comparison with the corresponding trajectory makes it clear that the actual penetration is far more. That is, more than that expected from a steady jet having a velocity equal to $2U_j$. Thus, the result of the periodic forcing is not simply a quasi-steady effect and there are ‘dynamic’ effects involved.

An observation of Fig. 2 makes it apparent that there is an organization and reinforcement of the shear-layer vortices. Cross-sections of distinct vortex rings are visible. Each vortex ring propels deeper into the crossflow due to self induction. The effect here is similar to that in a synthetic jet (SJ).¹² Note that a SJ in a crossflow (SJCF) is similar to an oscillatory JICF albeit with $U_j = 0$. Forcing frequencies for a JICF that yielded higher penetration and mixing in past studies,⁸⁻¹⁰ correspond to Strouhal numbers ($St = fD/U_j$) in the range of 0.1 – 0.5. The range brackets the jet ‘preferred mode’ Strouhal number. This reinforces the notion that the effect of the oscillatory blowing occurs primarily through an organization of the jet preferred mode (or shear layer) vortices.

While the result shown in Fig. 2 is encouraging from flow control and mixing enhancement perspective, another set of

data from Eroglu and Breidenthal’s work raises the possibility of a limitation. Figure 3 shows forcing effect at a higher jet Reynolds number. Here, the jet is turbulent as inferred from the smoke traces. It can be seen that the penetration for the forced case is not deeper than the trajectory expected from the peak velocity within the cycle. Nevertheless, it should be recognized that a net gain has been achieved with the forcing. The jet has penetrated to a depth expected of the maximum velocity within the cycle ($2U_j$) with half the mass flow rate (corresponding to U_j). For a SJCF also it has been shown that the penetration and jet trajectory correspond to the maximum velocity in the discharge half of the cycle.¹³ (While the SJCF is a subclass of oscillatory JICF, in view of the breadth of the subject, they are not included further in the discussion.)

Should the higher penetration of a forced JICF observed in Fig. 2 disappear at high Re when the jet becomes turbulent? The answer is not completely clear. However, as indicated earlier the preferred mode vortices are characteristic of jets with fully turbulent initial boundary layer and can just as well be organized by periodic forcing.^{4,14} Thus, a dynamic effect as in Fig. 2 is quite plausible with a turbulent JICF. Many aspects of the perturbation, e.g., frequency, amplitude, wave shape and duty-cycle come into play. For a forced JICF, the effects of these parameters and their interdependence are not fully understood yet. The latter aspects have been explored in some detail in Ref. 9 as well as 7, as discussed next.

Figure 4 shows selected flow visualization pictures from M’Closkey *et al.*⁹ The forcing function is a square-wave and compensated to ensure a square-wave response at the orifice exit. The pictures exhibit a similar effect as in Fig. 2. (The jet discharge here is up and normal to the floor. This will be the case for the rest of the paper.) The forcing is effective within a range of frequency and ineffective outside that range. The frequencies 55 Hz and 110 Hz correspond to Strouhal numbers of 0.13 and 0.27, respectively. The duty-cycle (i.e., the fraction of the period over which the high velocity occurs) has apparently been varied to obtain a pronounced effect. The duty-cycle for the 55 Hz case is 15% while that for the 110 Hz case is 31%. Obviously these parameters determine the strength and spacing of the periodic vortices. For a JICF not only the forcing has to produce the vortex rings with concentrated vorticity but they also need to be spaced optimally so that self and mutual induction are most effective for deeper penetration. Intriguingly, Ref. 9 reports compensated sine waves to be ineffective. It is intriguing because most previous studies on synthetic jets as well as forced free jets have involved sine-wave perturbation.

It suffices to say that there are many unknowns at this time. Thus, the difference observed between Figs. 2 and 3 may be due to other factors rather than due only to a difference in the state, viz., laminar versus turbulent. Clearly, more work is desirable exploring the forcing effects especially at higher Reynolds number.

2.2 Wake vortices and a mechanical perturbation:

The wake vortices are illustrated in Fig. 5, with two flow visualization pictures taken from Fric and Roshko.³ The picture at the top is a plan-view illustrating the Karman vortex like structures in the wake. If the ‘shedding’ were from a vertical

cylinder, each of these vortices would be a 'roll' parallel to the cylinder. The JICF is curved, thus, the vortex system is complex. The picture at the bottom is a side-view illustrating the curved shapes of the vortex rolls. Obviously, they span from the jet at the top to the wall underneath. Presumably, they connect the CVP and the vortex sheet of the wall boundary layer.

In shedding from a bluff body the vorticity source is the boundary layer on the body itself. A JICF is not a source of new vorticity. It is plausible that the wake vortices are a result of vorticity redistribution from the CVP and the shear layer. However, by tagging the fluid from the jet and the wall boundary layer separately Fric and Roshko inferred that the wake vortices in fact drew vorticity from the wall boundary layer. This constitutes a fundamental difference between the wake vortices and the shed vortices from a bluff body. Note in Fig. 5 that with increasing distance away from the jet there is amalgamation of the wake vortices – sometimes multiple – before they terminate on the wall boundary layer.

In connection with a study of JICF from asymmetric orifices Wu et al.⁵ presented a set of visualization pictures that deserves attention. These are reproduced in Fig. 6. Upon an inspection one may recognize strands of wake vortices in the picture at the top. (Note that the terminology used in Ref. 5 is 'spin-off' vortices.) The orifice used is of 'tear drop' shape that is also yawed relative to the free-stream. What is pertinent in the present discussion is the effect of a mechanical perturbation that is shown in the picture below. A small fin attached to the end of a rod is placed on the lee-side of the jet and oscillated periodically. The organization of the wake vortices downstream is unmistakable and remarkable. This has demonstrated that the wake vortices can be organized and made periodic. It is an aspect that has not been pursued any further to the author's knowledge. Clearly, a further exploration of the process and its impact on mixing enhancement is also desirable.

3. EXPERIMENT ON EFFECT OF OSCILLATING TABS

A mechanical perturbation technique, under exploration, is described in this section. It appears to work through a direct influence on the CVP. Results for an isolated JICF, presented earlier,¹⁵ are reviewed first beginning with the observations that led to the concept.

In previous investigations^{16,17} stationary vortex generators in the form of triangular tabs were tried in an effort to increase mixing and penetration of a JICF. This was prompted by earlier success with tabs in increasing mixing of free jets.¹⁸ For a JICF, it was thought that a tab placed on the downstream edge of the orifice, relative to the direction of the crossflow, would be effective. For then the vortex pair generated by the tab would be of the same sign as the CVP. This would reinforce the CVP that in turn would cause an increased jet penetration. However, results of Refs. 16 and 17 made it clear that the flow was practically oblivious of the presence of the tab in that configuration. Figure 7 is reproduced from Ref. 17. Mean velocity distribution on a cross-sectional plane is shown; the relevant tab configurations are indicated by the inserted sketches. The two sets of data on the top exhibit the lack of effect when the tab is placed on the leeward side. The ineffectiveness was qualitatively attributed to the

existence of a 'pressure valley' on the leeward side; for further details the reader is referred to the cited paper.

During the course of the experiments of Ref. 17 certain other tab configurations produced effects worthy of consideration. For example, when the tab was placed on the windward side a reduction in the jet penetration was achieved that may be of interest in film-cooling type application. This effect can be seen at the bottom right of Fig. 7. An explanation for the reduced penetration lies in the weakening of the CVP caused by the tab vortex pair that now has a sense opposite to that of the CVP.

Of relevance to the current study is the result shown at the bottom left of Fig. 7. Here, two tabs were placed at the 90° and 270° positions relative to the direction of the crossflow. The intent was to place the tabs symmetrically. However, a slight asymmetry in the placement upset the flowfield drastically. The core of high-speed fluid tilted on one side, as can be seen. Later, it was determined that if the asymmetry was reversed deliberately the tilt occurred the other way.

This led to the thought that a periodic reversal of asymmetry in two such tabs would result in a side-to-side swaying motion of the jet that might invigorate mixing. The oscillation of the tabs would be between a 'counter-clockwise' (CCW) configuration, as shown in Fig. 8, and the reversed 'clockwise' (CW) configuration. Results of such perturbation for an isolated JICF, presented in Ref. 15, are summarized in the following. First, the experimental procedure is briefly described.

3.1 Experimental procedure:

The experiments were conducted in a low-speed wind tunnel with a 30 x 20 inch (76.2 x 50.4 cm) test section. The jets discharged from 3/4 inch (1.9 cm) diameter (D) orifices. The orifices were located on a rectangular plate that was flush mounted on the test section floor. The tab oscillation mechanisms were housed underneath the plate. A picture of the set-up is shown in Fig. 9. Each orifice had two 'relays'. The tabs, mounted on the shafts of the relays, could be subjected to angular displacement at desired frequencies up to 80 Hz.

The jet flow was provided through a common plenum chamber that branched off into three supply lines to the orifices. There were two flow conditioning screens per orifice. Hot-wire surveys were first conducted to ensure that the velocity at the exit of each orifice was the same for a common supply pressure. This required fine adjustment of the length of the feed tubes. An orifice meter fitted to the supply line monitored the mass flow rate. With the assumption that the flow divided equally among the three orifices, the average jet velocity (U_j) was determined.

The three orifices, spaced $6D$ apart, were aligned perpendicular to the direction of the crossflow. For the following data, the coordinate origin is at the center of the central orifice. Streamwise (in the direction of crossflow), transverse (perpendicular to the floor) and spanwise directions are denoted by x , y and z , respectively. Hot-wire surveys were conducted with two adjacent X-probes. This provided distributions of all three components of velocity, time-averaged as well as phase-averaged. The experimental set-up in Ref. 15 was identical to the description above except that it involved only one orifice. An

interested reader may look up this reference for further details of the tab oscillation mechanism and measurement procedures.

3.2 Summary of results in Ref. 15:

Figure 10 shows phase-averaged streamwise velocity at $x/D = 8$ for four different phases. The phases are approximately equally spaced within the oscillation cycle. The purpose here is to provide an overall picture without details of the data. It can be seen that the periodic perturbation indeed swayed the jet side-to-side providing a proof of the concept. Figure 11 shows corresponding phase-averaged streamwise vorticity distributions. The CVP is visible and the effect of the perturbation is also clear. One branch of the CVP gets accentuated periodically while the other gets weakened as it is lifted up. Thus, the effect of the tab oscillation may be viewed as a direct perturbation of the CVP.

Parametric dependence of the flow response was investigated. It was found that the technique was effective only at high J with little or no effect at J less than about 15. Above that threshold, however, the effect became more pronounced with increasing J . At $J = 48$, detailed surveys were conducted. The flow oscillation persisted as far downstream as the measurements were permitted by the facility ($x = 100D$). The flow responded to the oscillation in a low frequency range. The fundamental amplitude measured at a fixed location was approximately constant up to about 25 Hz. At higher frequencies the amplitude dropped off rapidly. Thus, the effective frequency range was low – more than an order of magnitude lower than the preferred mode Strouhal number. It was also found that the unsteady disturbance propagated downstream approximately at the speed of the crossflow (U_∞).

3.3 Results for an array of three orifices:

An examination of the time-averaged flowfield in Ref. 15 indicated a modest increase in mixing and jet spreading under the tab oscillation. It was conjectured that the effect would be accentuated with an array of orifices. Appropriate phasing of the perturbation for the adjacent orifices might result in a beneficial interaction of the CVP's yielding enhanced mixing. This led to further experiments. Preliminary results are discussed in this section.

Time-averaged flowfield for the central orifice only are first shown in Fig. 12. The two tabs are stationary and placed symmetrically. The mean velocity field is as expected of a JICF, with a 'kidney shaped' distribution of the high momentum fluid. The streamwise vorticity distribution quantifies the intensity of the CVP. The turbulence intensity (u') data exhibit that the highest turbulent activity coincides with the cores of the CVP.

The flowfield for the array of three JICF, each run at the same J and Re_j as in Fig. 12, is shown in Fig. 13. All three orifices have stationary tabs placed approximately symmetrically. The central jet and parts of the outer jets are captured within the measurement range. Relative to the isolated jet case (Fig. 12) large changes are observed. The extent of the central jet has shrunk due to the influence of the side jets. Mean velocity distribution exhibits pockets of low and high momentum fluid. This is obviously due to imperfections in the placement of the stationary tabs. The vorticity amplitudes for the CVP are lower with cores staying closer to the wall. The turbulence intensity

distribution exhibit similar changes as noted for the mean velocity.

Corresponding data for the triple JICF are shown in Fig. 14, for $x/D = 12$, providing an idea about the flowfield evolution. The distributions are similar as at $x/D = 8$ (Fig. 13) with persisting nonuniformities. At $x/D = 12$ the peak amplitudes of all properties have decreased significantly. Note that instead of u' the w' -component of turbulence intensity is shown in Fig. 14. The latter component was influenced most by a specific case of tab oscillation described next.

The three pairs of tabs were oscillated at 4 Hz in phase. That is, all three were swept in the same angular direction at a given instant. Thus, all three pairs would be CCW or CW simultaneously. Time-averaged data obtained at $x/D = 12$ are shown in Fig. 15. The effect of the perturbation can be appreciated by comparing with data in Fig. 14. There are significant changes. Some of the nonuniformities in the mean velocity field have been smoothed out. Vorticity magnitudes for the CVP have dropped. The spanwise turbulence intensity (w') is significantly larger. For this oscillation case, the changes in either u' - or v' -fields (not shown for brevity) was not as dramatic. Thus, in this case strong spanwise fluctuations have been introduced.

In order to assess the overall impact of the perturbation the following integral quantities were calculated. With all velocities normalized by the freestream velocity, U_∞ and A being the area of the domain,

$$C = \frac{1}{AU^2} \int (U(y, z) - \bar{U})^2 dydz,$$

where,

$$\bar{U} = \frac{1}{A} \int U(y, z) dydz,$$

and

$$k = \text{SQRT} \left(\frac{1}{A} \int (u'^2 + v'^2 + w'^2) dydz \right).$$

The quantity 'C' is a measure of spatial nonuniformity in the U -distribution, while k represents total turbulence intensity averaged over the domain. In order to avoid a bias due to the sharp gradients the wall boundary layer was excluded from the integration domain.

Streamwise variation of C and k based on data at $x/D = 8, 12$ and 16 arc shown in Fig. 16. The case 'osc0' denotes unperturbed flowfield as in Figs. 13 and 14. The case 'osc2' denotes the in-phase oscillation of Fig. 15. The case 'osc3' denotes another oscillation case where the middle pair of tabs was 180° out of phase with respect to the two outer pairs. For the latter case only one set of data was acquired at $x/D = 12$. (It was noted that 'osc3' introduced stronger transverse fluctuation resulting in larger v' intensity with little change in w' , in contrast to the effect of 'osc2' discussed earlier.) One finds that the overall intensity (k) has increased at all streamwise locations under the perturbation. The relative increase is more at farther downstream locations. The percentage increase in k with perturbation is more at $x/D = 16$ than at 8. Note also that the net impact on k is similar for the two oscillation cases.

The spatial nonuniformity index C has decreased at all stations under the perturbation. An increased mixing has resulted in a more uniform flowfield. As with k , the relative change in C is more with increasing distance downstream. Thus, the effect of the perturbation has become increasingly pronounced with increasing distance downstream, within the measurement range. This is a consequence of the fact that the underlying periodicity persists far downstream, via a modulation of the CVP. Thus, at this point, the technique appears not to be attractive for applications demanding fast and immediate increase in mixing. On the other hand, it may be attractive for applications that require a persistent increase of mixing sustained over a long distance. Alleviation of massive flow separation and management of secondary flow could be examples of such application.

4. CONCLUDING REMARKS

In this paper effects of periodic perturbation on a jet in a crossflow are reviewed. Flow visualization pictures from several past works are discussed. Different vortex systems of a steady JICF are first identified. It is reasoned that specific perturbation techniques work through an organization of specific vortex systems. Thus, oscillatory blowing works through an organization and intensification of the jet shear layer (or preferred mode) vortices. On the other hand, a mechanical perturbation applied on the lee-side of the JICF is found to organize the wake vortices.

Oscillatory blowing increases jet penetration significantly. The increase is more than that expected simply from peak velocity within the oscillation cycle. The effect is most pronounced at low Reynolds numbers when the jet is 'laminar'. The penetration is found to be less at higher Reynolds number when the jet is 'turbulent'. It is reasoned that the apparent influence of the state of the jet is not conclusive. There are many parameters of the forcing function that come into play. The impact of the individual parameters and their interdependence are not clearly understood yet.

Results of another mechanical perturbation technique from a current experiment are presented. This involves a pair of tabs at the exit of the jet orifice. An asymmetry in the placement of the tabs is reversed periodically. This directly modulates the CVP. With reference to the discussion of Fig. 6 a question arises if this technique also organizes the wake vortices. This aspect has remained unexplored. The impact on the CVP, however, is clear and demonstrated by phase-averaged measurement of streamwise vorticity. The effect of the perturbation persists as far downstream as the measurements are permitted by the facility (100 diameters from the orifice). The persistent effect occurs since the CVP also persists in the flow.

The technique is applied to an array of three orifices. The flowfield downstream is surveyed to provide distributions of mean velocity, streamwise vorticity and turbulence intensities. An improved uniformity in the cross-sectional distribution of mean velocity occurs under the perturbation. Overall turbulent kinetic energy, integrated over the cross-section, is also higher in the perturbed case. The relative difference between the perturbed and unperturbed cases, both in terms of flow uniformity and turbulent kinetic energy, become more pronounced with increasing distance downstream. This is also due to the persistence of the coherent perturbations in the flowfield via the modulation of the CVP.

ACKNOWLEDGEMENT

The author is grateful to the NASA Quiet Aircraft Technology (QAT) Program for support during this work. The work was partially supported by Army Research Laboratory Director's Research Initiative (DRI) Program.

REFERENCES

- [1] Seifert, A. and Pack, L.G., "Active control of separated flow on a wall-mounted "hump" at high Reynolds numbers", *AIAA J.*, **40** (7), pp. 1363-1372, July, 2002.
- [2] Miller, D.N., Yagle, P.J., Bender, E.E., Smith, B.R. and Vermuelen, P.J., "A computational investigation of pulsed injection into a confined, expanding crossflow", *AIAA Paper* 01-3026, 31st Fluid Dynamics Conference, Anaheim, CA, June, 2001.
- [3] Fric, T. F. and Roshko, A., "Vortical structure in the wake of a transverse jet", *J. Fluid Mechanics*, **279**, pp. 1-47, 1994.
- [4] Crow and Champagne, "Orderly structures in jet turbulence", *J. Fluid. Mechanics*, **48**, p. 547, 1971.
- [5] Wu, J.M., Vakili, A.D. and Yu, F.M., "Investigation of the interacting flow of nonsymmetric jets in crossflow", *AIAA J.*, **26**(8), pp. 940-947, 1988.
- [6] Vermeulen, P.J., Chin, C.-F. and Yu, W.K., "Mixing of an acoustically pulsed air jet with a confined crossflow", *J. Propulsion*, **6**(6), pp. 777-783, 1990.
- [7] Johari, H., Pacheco_Tougas, M. and Hermanson, J.C., "Penetration and mixing of fully modulated turbulent jets in crossflow", *AIAA J.*, **37**(7), pp. 842-850, 1999.
- [8] Eroglu, A. and Breidenthal, R.E., "Structure, penetration, and mixing of pulsed jets in crossflow", *AIAA J.*, **39**(3), pp. 417-423, 2001.
- [9] M'Closkey, R.T., King, J.M., Cortelezzi, L. and Karagozian, A.R., "The actively controlled jet in crossflow", *J. Fluid Mechanics*, **452**, pp. 325-335, 2002.
- [10] Narayanan, S., Barooah, P. and Cohen, J.M., "Experimental study of the coherent structure dynamics & control of an isolated jet in cross flow", *AIAA Paper* 02-0272, 40th Aerospace Sciences Meeting, Reno, NV, Jan 14-17, 2002.
- [11] Abramovich, G.N., "The theory of turbulent jets", *The M.I.T. Press*, 1963.
- [12] Smith, B. L., and Glezer, A., "The Formation and Evolution of Synthetic Jets," *Physics of Fluids*, **10**(9): 2281-2297, 1998.
- [13] Milanovic, I.M. & Zaman, K.B.M.Q., "Synthetic jets in cross-flow Part 2 - jets from orifices of different geometry", *AIAA Paper* 03-3715, 33rd AIAA Fluid Dynamics Conf., Orlando, FL, June 23-26, 2003.
- [14] Zaman, K.B.M.Q. & Hussain, A.K.M.F., "Natural large-scale structures in the axisymmetric mixing layer", *J. Fluid Mechanics*, **138**, pp. 325-351, 1984.
- [15] Zaman, K. B. M. Q., "Effect of oscillating tabs on a jet-in-cross-flow", *AIAA Paper* 03-0632, 41st AIAA Aerospace Sciences Meeting, Reno, NV, January, 2003
- [16] Liscinsky, D.S., True, B. and Holdeman, J.D., "Effects of initial conditions on a single jet in crossflow", *AIAA Paper* 95-2998, 31st Joint Propulsion Conference, San Diego, July 10-12, 1995.

- [17] Zaman, K.B.M.Q. and Foss, J.K., "The effect of vortex generators on a jet in a cross-flow", *Physics of Fluids*, 9 (1), pp. 106-114, 1997.
- [18] Zaman K.B.M.Q., Reeder M.F., & Samimy M., 1994, "Control of an axisymmetric jet using vortex generators", *Physics of Fluids A*, 6 (2), pp. 778-793.

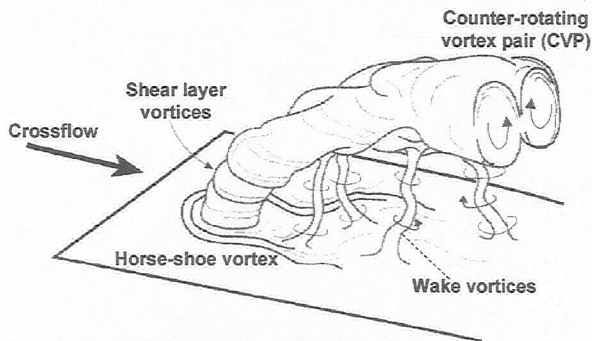


Fig. 1 Schematic of vortex systems of a jet in a crossflow, from Fric & Roshko (1994).³

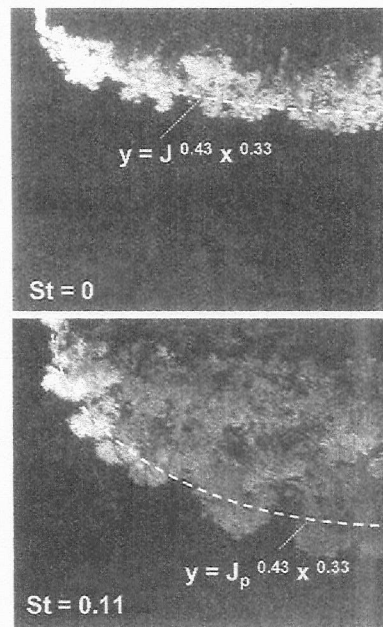


Fig. 3 Flow visualization pictures of a pulsed JICF, similar to those in Fig. 2, at $Re_J = 6200$; Eroglu and Breidenthal (2001).⁸

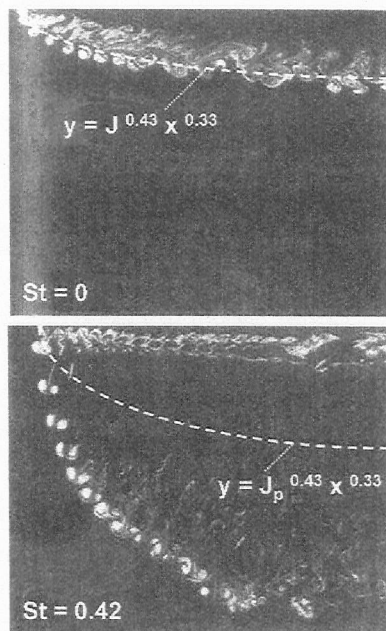


Fig. 2 Flow visualization pictures from Eroglu and Breidenthal (2001)⁸ for a pulsed JICF at indicated Strouhal numbers (St); $Re_J = 650$, $J = 5.3$. Superimposed dashed lines are approximations of indicated equations for jet trajectories. Momentum flux ratios, J and J_p , are based on mean jet velocity (U_j) for the unpulsated case and peak velocity (U_p) for the pulsed case, respectively.

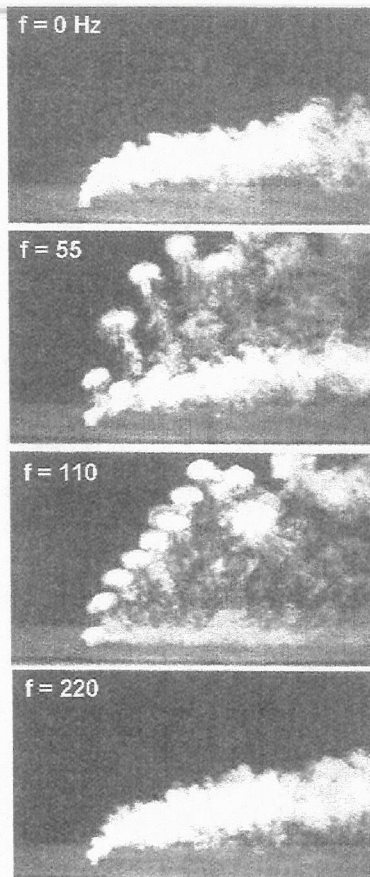


Fig. 4 Flow visualization pictures of a JICF pulsed with 'compensated' square-wave with controlled 'duty-cycle' at indicated frequencies (Hz) from M'Closkey, King, Cortelezzi and Karagozian (2002);⁹ $Re_J \approx 1600$, $J = 6.7$.

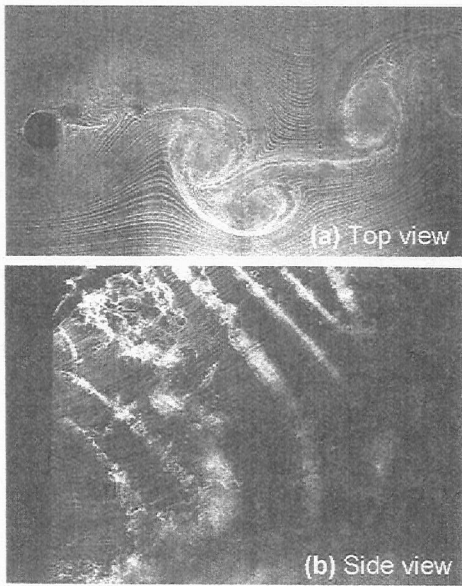


Fig. 5 Flow visualization pictures illustrating wake vortices; Fric and Roshko (1994).³ (a) Horizontal smoke wire at $0.5D$ from floor, $Re_J = 45,000$, $J = 16$, (b) vertical smoke wire at $6D$ downstream from orifice, $Re_J = 114,000$, $J = 100$.

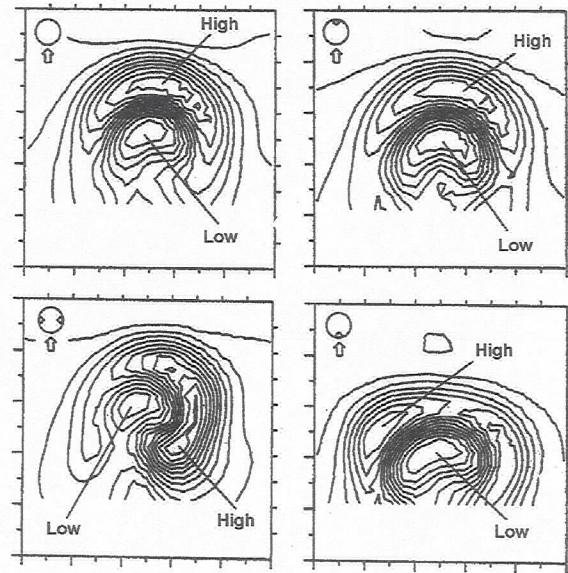


Fig. 7 Effect of tab(s) on mean velocity distribution of a JICF at $x/D = 4$, from Zaman & Foss (1997).¹⁷ $Re_J = 46,000$, $J = 21$.

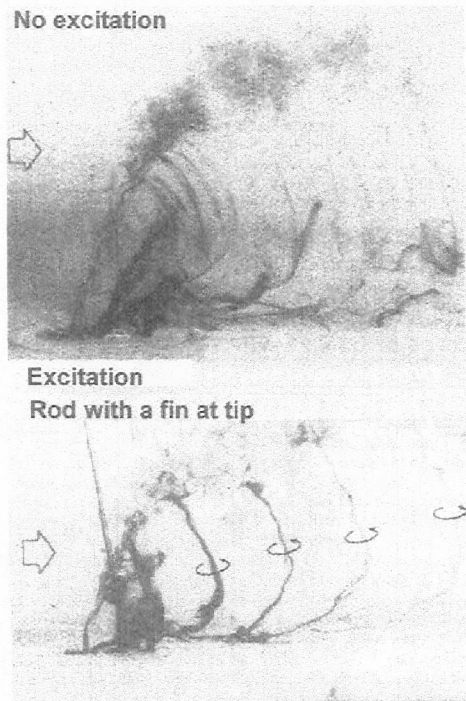


Fig. 6 Flow visualization pictures from Wu, Vakili and Yu (1988)⁵ demonstrating controllability of the wake vortices by perturbation; $Re_J = 540$, $J = 6.25$.

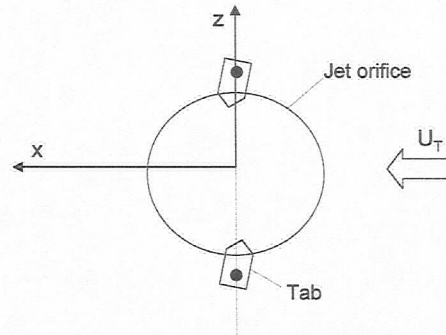


Fig. 8 Schematic of oscillating tab arrangement. Two tabs are in extreme counter-clockwise (CCW) position.

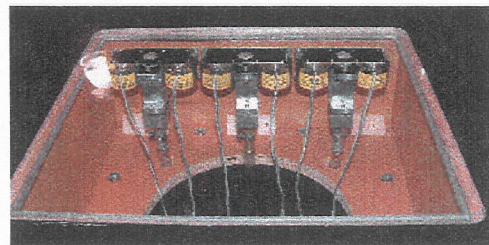


Fig. 9 Picture of triple JICF apparatus with oscillating tab mechanisms.

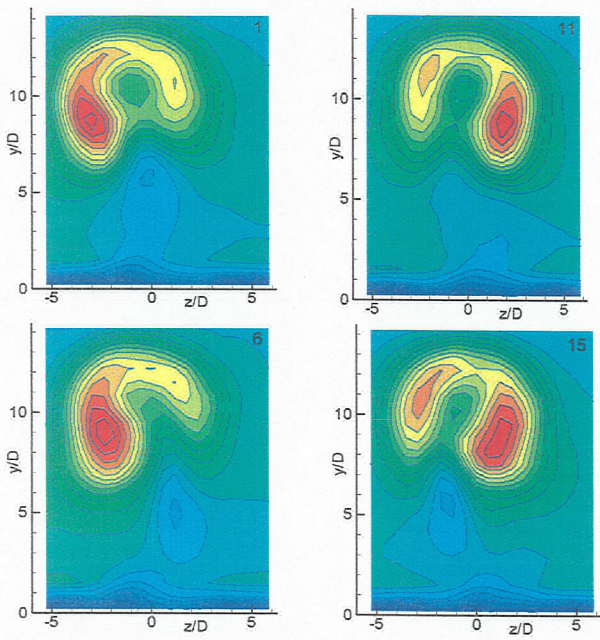


Fig. 10 Cross-sectional distributions of phase-averaged streamwise velocity, for four different phases within the (8 Hz) oscillation cycle; $x/D = 8$, $Re_J = 57,000$, $J = 48$; from Zaman.¹⁵

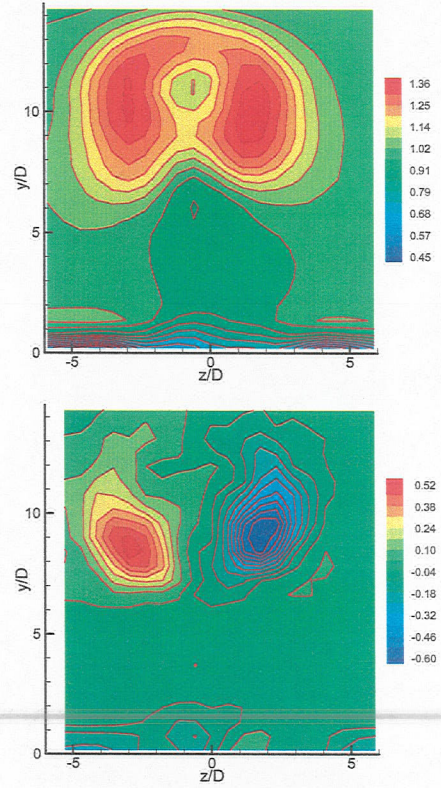


Fig. 12 Flow field of Single JICF with 2 symmetrically placed stationary tabs; $x/D = 8$, $Re_J = 42,000$, $J = 45$. Top: mean velocity U/U_∞ middle: streamwise vorticity, $\omega_x D/U_\infty$, bottom: turbulence intensity, u'/U_∞ .

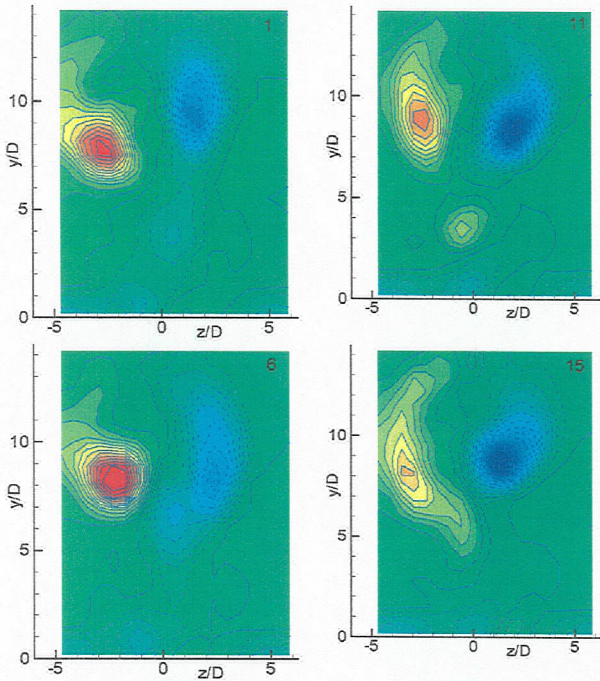


Fig. 11 Phase-averaged streamwise vorticity ($\omega_x D/U_\infty$), corresponding to the data of Fig. 10.

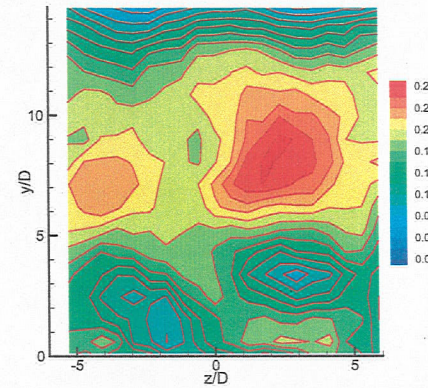
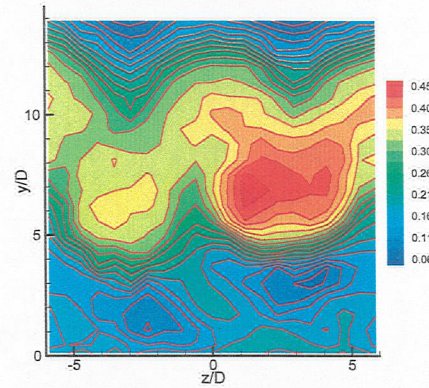
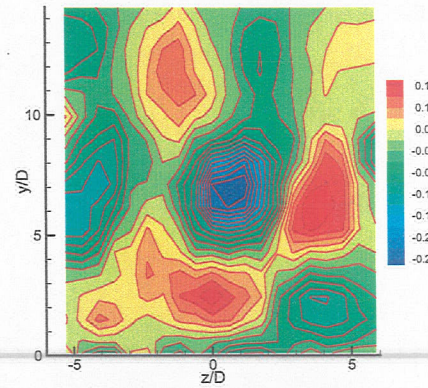
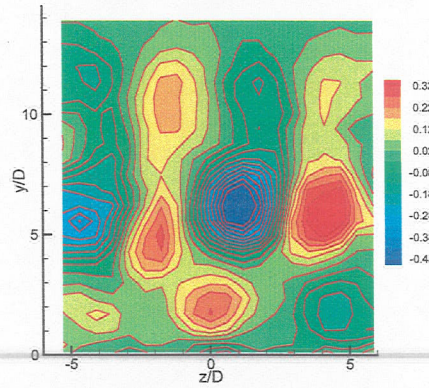
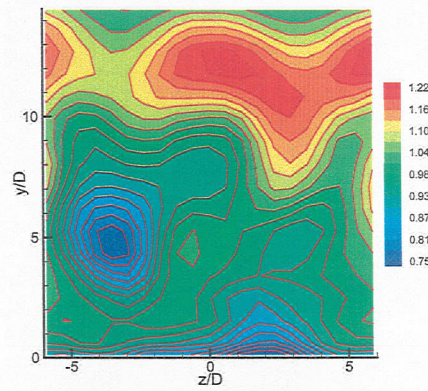
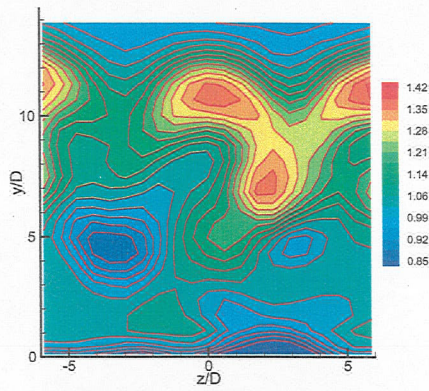


Fig. 13 Data corresponding to Fig. 12 capturing the central domain of the triple JICF. Each orifice has 2 symmetrically placed stationary tabs; $x/D = 8$, $Re_J = 42,000$, $J = 45$. Top: mean velocity U/U_∞ middle: streamwise vorticity, $\omega_x D/U_\infty$, bottom: turbulence intensity, u'/U_∞ .

Fig. 14 Data corresponding to Fig. 13 at $x/D = 12$. Top: mean velocity U/U_∞ middle: streamwise vorticity, $\omega_x D/U_\infty$, bottom: turbulence intensity, w'/U_∞ .

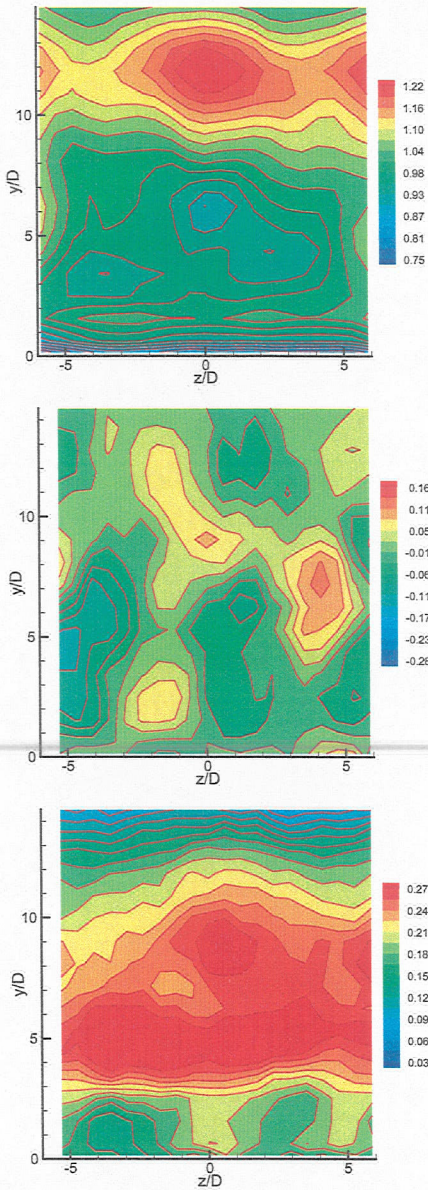


Fig. 15 Flowfield of triple JICF with all pairs of tabs oscillated in sync at 4 Hz, $Re_J = 42,000$, $J = 45$, $x/D = 12$. Top: mean velocity U/U_∞ , middle: streamwise vorticity, $\omega_x D/U_\infty$, bottom: turbulence intensity, w'/U_∞ .

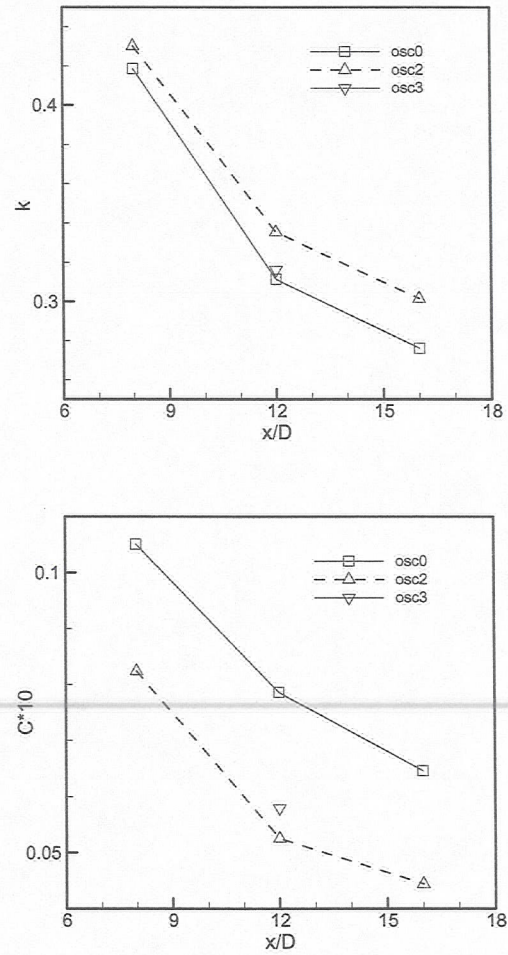


Fig. 16 Integral of total turbulence intensity (k) and rms of spatial nonuniformity in mean velocity (C) from field data as in Figs. 14 and 15. Oscillation cases: 'osc0' = stationary tabs; 'osc2' = all pairs oscillated in sync at 4 Hz; 'osc3' = oscillation at 4 Hz with central pair 180° out of phase relative to the two outer pairs.